PHYSICAL REVIEW D VOLUME 42, NUMBER 9 1 NOVEMBER 1990

Quantum correlations in high-energy multihadron distributions

Chia C. Shih
Department of Physics, University of Tennessee, Knoxville, Tennessee 37966-1200
and Department of Physics and Center for the Study of Complex Systems, University of Arizona, Tucson, Arizona 85721
(Received 7 October 1988; revised manuscript received 6 August 1990)

We have used the Jaiswal and Mehta formulation as a model of hadronic multiplicity distributions to evaluate the joint forward-backward multiplicity distribution $P(N_F,N_B)$ in hadronic interactions, where the underlying field includes a mixture of a coherent component and Gaussian noise. This allows us to investigate the effect of the quantum correlation length in rapidity on the strength of the forward-backward correlation, the validity of the binomial distribution for fixed N_F+N_B, and the Koba-Nielsen-Olesen distribution. The resultant parameters indicated that for the NA22 and CERN ISR regions, the relative noise content rises slowly with energy, while the correlation length also increases with the total width of the rapidity window.

I. INTRODUCTION

Recently there has been continuing interest in the stochastic nature of the multiplicity distribution in hadronic production at high energies. The statistics of the many-hadron system have been introduced into the phenomenology at various stages of data interpretation.[1–3] Recent consideration of "intermittency"[4–9] and its interpretation is a perfect example of demonstrating the differences in approaches between "dynamics" and statistics. Eventually, the fundamental motivation of all the approaches should be not only to investigate the underlying dynamics, but also to understand the nature of the statistics of strongly interacting systems.

Generally speaking, in a "dynamical" approach one assumes that the hadronic production process is so energetic and chaotic that the system can essentially be described classically. Good examples are the string dynamics used in the Lund FRITIOF model,[10] dual topological unitarization,[11,12] and the geometrical picture in impact-parameter smearing[13] (IPS) models. Quantum-mechanical relations enter through the unitarity condition and the final-state interaction of hadronization. Other quantum-mechanical aspects, related to the correlation and fluctuation of the production process, are more difficult to incorporate into these classical considerations.

The existence of quantum-mechanical effects in hadronic production processes are demonstrated beyond doubt with the observation of the Bose-Einstein effect in the final state of like pions.[14] Since soft-pion production is a dominant production process, and since the wave function of soft pions may overlap substantially, a quantum stochastic description of the production processes should be considered seriously. It is otherwise difficult to estimate possible systematic biases in many production mechanisms which are intrinsically semiclassically oriented.

In the "statistical" approach, the production process is formulated essentially as a quantum or classical stochastic system.[1–3] To start with, however, there is no *a priori* assumption that the strongly interacting dynamics is classical at high energy and high density. Correlations and fluctuations of the probability distribution may therefore be strongly influenced by the overlap of the amplitudes.[15] By retaining the quantum-mechanical formulation, one hopes to understand when, and if, classical stochastic formulations such as the string dynamics, or geometry picture can be good approximations of the system. Distinctions between the classical and quantum-mechanical characteristics may not depend crucially on the detailed dynamics of the soft-hadron system. The situation for hadron physics is similar but more uncertain than that in the early stages in quantum optics.[16,17] (For extensive reviews of these aspects of quantum optics, we refer to the excellent reviews by Saleh[18] and Perina[19].)

Quantum statistical properties of a coherent signal mixing with Gaussian stochastic noise has been investigated since the 1960s.[20–27] Most of the work in this area was done by researchers who were interested in the characteristics of quantum statistics in photoelectron counting. Fowler and Weiner later introduced the same formalism to high-energy hadronic interactions, and suggested a strong analogy between the time t and the rapidity y.[28,29] A similar formulation was also developed by Gyulassy for nuclear collisions.[30] However, differences exist between the hadron and photon systems. For example, unlike photons, some of the final-state pions are charged.[31–33] The statistics of the hadronic system are also evaluated eventwise, with energy and other conservation laws playing a role. The statistics of the hadronic finite system may therefore be different than the usual stationary problem in quantum optics.

Recently Fowler *et al.* have used the factorial cumulant in conjunction with the hadronic leading-particle effect to study phenomenology in hadronic multiparticle production.[34] Their result demonstrates the usefulness of the statistical approach. In order to digest and convey in a more concrete way the results of these types of analysis, it is desirable to go beyond the factorial cumulant and construct joint hadronic multiplicity distributions between different regions. This is in fact not an easy task. Even in quantum optics, there are only a few analytic expressions for the probability distributions.

In order to bridge the gap between the semiclassical dynamics and the quantum statistics approaches, it is necessary to investigate in more detail the specific underlying structure of the typical quantum statistical approach such as the models used by Fowler *et al.* On one hand, an analysis along this line allows us to expand the predicative power of the quantum statistical approach beyond the factorial cumulant and the forward-backward correlation slope parameter. On the other hand, it also suggests a specific direction in extending classical models to incorporate possible quantum statistical effects. What we shall present here is an explicit translation of the quantum statistical formulation, which is often used in quantum optics, to the study of hadronic multiplicity distributions. We shall adopt specifically the Lorentzian spectrum as the quantum optical correlation function. Some of the basic properties of this correlation function can be found explicitly in quantum optics, and are adopted directly for hadronic physics. Much of the phenomenological analysis of the hadronic distributions discussed below is, however, beyond the common scope of quantum optics.

In this paper we shall investigate the multiplicity distribution in a single region and their correlations in different regions. In order to avoid excessive numerical details and to focus on the essentials, we shall ignore the differences between the hadronic and photon production processes. Instead we shall emphasize the global properties of the correlation which are not often addressed in quantum optics, but are examined frequently in hadronic physics. This includes features such as the Koba-Nielsen-Olesen (KNO) distributions, forward-backward correlation, and the effective cluster size.

In the following, we shall briefly review the basic formulation of the multiplicity distribution in order to extend the distributions usually measured in hadron physics. What has been available in the literature up to now is only the low-order factorial cumulant of the overall distribution. The generalization to the probability amplitude discussed in this paper is conceptually very simple. What we shall present here is the numerical evaluation of the joint forward-backward probability distribution $P(N_F,N_B)$. As a result we are able to compare the multiplicity distribution of $N_S=N_F+N_B$ directly with the data. We are also able to examine more explicitly the dependence of $\langle N_B\rangle_F$ on N_F. The resultant total χ^2's compare rather favorably with experimental data at NA22 (Ref. 35) and CERN ISR (Refs. 36 and 37) energies and are as good as other current phenomenological representations. Our present study therefore lays the groundwork for further studies that should eventually be carried out for a more comprehensive formulation of a quantum stochastic process, similar to what has been reported by Fowler *et al.*[34]

II. BASIC FORMULATION OF THE DISTRIBUTION

A. Multiplicity distribution for a single region

Multiplicity distributions are sensitive to coherence length and degree of freedom of the underlying stochastic process. Back in 1959, Mandel analyzed photon multiplicity distributions in terms of effective number of cells per unit time interval.[15] The multiplicity distribution of a Gaussian light can then be approximated by negative binomials without the detailed nature of the correlation spectrum. In order to study in more detail the shape of the multiplicity distributions and the correlation between different time intervals, it is, however, necessary to specify the explicit functional form of the spectrum function. Partial coherence also has to be included. In this paper, we shall confine ourselves to the class of the quantum-mechanical system with a Lorentzian spectrum of correlation. This is because the Lorentzian spectrum is one of the most natural spectrum of correlation. Detailed analysis of the moments of the distribution was also studied by Jaiswal and Mehta[26] (JM).

Traditionally in the JM formulation, the probability of n particles being registered in an interval (y_1,y_2), is given by[26]

$$P_n=\int_0^\infty \frac{W^n}{n!}e^{-W}P(W)dW \ . \tag{1}$$

Here W is the integrated intensity over the interval in y,

$$W=\int_{y_1}^{y_2} I(y)dy \ , \tag{2}$$

and $P(W)$ is the probability density of the random variable W. We shall now assume that conservation laws do not play an important role. Thus $I(y)$ is approximately a constant, independent of y. Furthermore, $I(y)$ may be described by a random field $V(y)$,

$$I(y)=|V(y)|^2 \ . \tag{3}$$

Characteristics of the stochasticity of the filed $V(y)$ shall be described in detail. At this moment, it is only necessary to notice that the probability P_n should be averaged over an ensemble of $V(y)$, thus

$$P_n=\left\langle \frac{W^n}{n!}e^{-W}\right\rangle_{\text{ensemble}} \ . \tag{4}$$

In a quantum statistical approach, the radiating field $V(y)$ may have a coherent and a chaotic part expressed through

$$V(y)=V_c(y)+V_r(y) \ . \tag{5}$$

Here the coherent field $V_c(y)$,

$$V_c(y)=V_0e^{-i(\omega_0 y+\phi)} \ , \tag{6}$$

has constant magnitude V_0 and a random phase ϕ [which eventually drop out of $I(y)$, and is therefore taken as real for our purpose]. $V_c(y)$ leads to a flat rapidity distribution. This is true if the system is in an eigenstate of the boost operator in y.[29] We are therefore making the assumption of stationarity in rapidity y. On the other hand, the random field $V_r(y)$ is defined as a complex Gaussian function through its first two moments

$$\langle V_r(y)\rangle_{\text{ensemble}}=0 \tag{7}$$

and

$$\langle V_r(y)^* V_r(y+y')\rangle_{\text{ensemble}} = \Gamma(y') \ . \tag{8}$$

All the higher-order correlation functions can be expressed through the second-order correlation function $\Gamma(y)$. Here $\Gamma(y)$ is an assumed to be given theoretically. It is a field correlation and cannot be measured directly. The validity of a specific choice of $\Gamma(y)$ is tested indirectly through the analysis of the correlation in the intensity $I(y)$ reflected in analyses of multiplicity distribution[38] or in Bose-Einstein effects.[39] We shall later on specifically take $\Gamma(y)$ to be Lorentzian, i.e.,

$$\Gamma(y_1,y_2) = \Gamma_0 e^{-i\omega_r(y_1-y_2)} e^{-\tau|y|} \ . \tag{9}$$

There are many dynamical models of the hadronic interaction in which the coherent and chaotic fields can be interpreted. For example, the hadronic field $V(y)$ can be the resultant hadronic field of an elemental current.[30] In this model of nuclear interferometry, a coherent field represents the collective effect of the current elements in different regions of space-time, while the chaotic field represents the incoherent contributions of the local currents at different space-time points. A physical interpretation along these lines may then lead to a space-time profile of the hadron. Alternatively, in a string type of model such as a Schwinger $(1+1)$-dimensional quantum-electrodynamics model or the symmetrical Lund model,[40] in the limit of high energy, the bound states of a charge pair are created as coherent states obeying a Poisson distribution in P_n. Its corresponding rapidity distribution is also a constant. Thus, the underlying field can be described by $V_c(y)$. Specify construction of the corresponding $V_r(y)$ in a string-type model remains an open question, which we are presently investigating. There are many possible sources of stochasticity. For example, the recent extension of the Lund model to incorporate hard-gluon scattering leads to a considerable amount of stochasticity in the otherwise coherent field.[5] In the first approximation, the overall field may become a superposition of the coherent and chaotic fields of partial coherence, as we describe in this paper. Instead of working at just the nature of the correlation function $\Gamma(y)$, we shall choose a Lorentzian form often used in quantum optics for the correlation of the chaotic field $V_r(y)$. The theoretical and statistical rationale for such a choice can be found in many references.[18]

Even with this well-known expression for $\Gamma(y)$, it remains very difficult to construct the probability distribution functions P_n analytically or numerically. We shall therefore outline a specific procedure in this paper. Let us expand the wave field V_r and V_c in an orthonormal base $\{\phi_m\}$:

$$V_r(y) = \sum_m C_m \phi_m(y) \ , \tag{10}$$

$$V_c(y) = \sum_m C_m^{(0)} \phi_m(y) \ , \tag{11}$$

where ϕ_m are the orthonormal eigenfunctions of the integral equation

$$\int_{y_1}^{y_2} \Gamma(y'-y)\phi_m(y')dy' = \lambda_m \phi_m(y) \ . \tag{12}$$

The uncorrelated random coefficients C_m satisfying

$$\langle C_m^* C_n \rangle = \lambda_m \delta_{m,n} \tag{13}$$

then possess a complex Gaussian distribution

$$P(\{C_m\}) = \prod_m \frac{1}{\pi\lambda_m} \exp\left[-\frac{|C_m|^2}{\lambda_m}\right] , \tag{14}$$

so that

$$\langle P_n \rangle_{\text{ensemble}} = \prod_m \int d\,\mathrm{Re}(C_m) d\,\mathrm{Im}(C_m) P(\{C_m\}) \frac{W^n}{n!} e^{-W} \ . \tag{15}$$

With this base, W is simply given by

$$W = V_0^2 Y + \sum_m (|C_m|^2 + C_m^{(0)} C_m^* + C_m^{(0)*} C_m) \tag{16}$$

$$= \sum_m |C_m + C_m^{(0)}|^2 \ , \tag{17}$$

the $\{C_m\}$ average can then be integrated analytically. We get

$$P_n = \sum_{\{n_m\}} \prod_m P_{n_m}^{\mathrm{GL}}(N_m, S_m) \delta\left[\sum n_m - n\right] ; \tag{18}$$

$$N_m = 1/(1+\lambda_m) \ , \qquad S_m = C_m^{(0)} \lambda_m / (1+\lambda_m) \ , \tag{19}$$

where P_n^{GL} is Glauber-Lachs distribution in quantum optics and is also often referred as the partially coherent laser distribution[1] (PCLD) with $k=1$,

$$P_n^{\mathrm{GL}}(N,S) = P_n^{\mathrm{PCLD}}(N,S,k=1)$$
$$P_n^{\mathrm{PCLD}}(N,S,k) = \exp\left[-\frac{S}{1+N/k}\right] \frac{(N/k)^n}{(1+N/k)^{n+k}} \times L_n^{k-1}\left[-\frac{kS/N}{1+N/k}\right] . \tag{20}$$

Here L_n^{k-1} is the generalized Laguerre polynomial of order $k-1$. Expressing P_n alternatively in terms of the generating function $G(s)$, we get

$$G(x) = \sum_0^\infty (1-x)^n P_n = \exp(-x\langle n_c\rangle) \prod_m \frac{1}{1+x\lambda_m} \times \exp\left[\frac{\langle n_c\rangle |f_m|^2 x^2 \lambda_m}{(y_2-y_1)(1+x\lambda_m)}\right] , \tag{21}$$

where

$$\langle n_c \rangle = (y_2 - y_1) V_0^2 \ . \tag{22}$$

Thus the JM formulation can be considered as the convolution of an infinite number of GL distributions. The existence of this relationship is not accidental. It followed from the fact that the statistical measure of our functional basis for the chaotic field is assumed to be Gaussian. As a consequence, the coherent part of the field, which is a constant field under the statistical average, leads to a displaced Gaussian distribution. Since the Karhunen-Loéve basis of expansion $\{\phi_m(y)\}$ diagonalizes the correlation spectrum function, the expansion coefficients $\{C_m\}$ are all statistically independent. However, the combined contributions of all the components lead to a flat and stationary chaotic correlation spectrum.

The requirement of the Lorentzian spectrum shape demands a specific statistical weight for each eigenfunction. In this sense, the overall probability distribution P_n can be evaluated most easily in this fashion. On the other hand, since P_n is only an overall convolution, it is difficult to characterize uniquely the difference between JM formulation and many other models that are constructed with or without any assumption on correlation. The real feature of JM model as compared to other models is therefore based on the correlation between different physical regions that we shall discuss in the next section.

B. Factorial cumulants

Instead of evaluating the probability distribution P_n directly, it is advantageous to investigate directly the properties of the functional space spanned by the orthonormal base through the factorial cumulants.[26,27] Numerical analysis is, however, often needed for a successful implementation of the procedure, because the difficulties in manipulating overlapping integrals of the orthonormal functions. To avoid the difficulties, it is convenient to start with the factorial cumulant generating function $H(x)$ given by the relation

$$H(x)=\ln G(1-x)=\sum_{k=1}^{\infty}(-x)^k\mu_k/k!$$

Substituting the definition of λ_m of Eq. (21) into the above equation, and integrating over the parameter space of the C_m, we obtain

$$\mu_k=(k-1)!\langle n_r\rangle^k B_k+k!\langle n_r\rangle^{k-1}\langle n_c\rangle\bar{B}_k \tag{23}$$

$$B_k=\int dy_1\Gamma^{(k)}(y_1,y_1) , \tag{24}$$

$$\bar{B}_k=\int dy_1\int dy_2 e^{i\omega_c(y_1-y_2)}\Gamma^{(k-1)}(y_1,y_2) , \tag{25}$$

$$\langle n_c\rangle=(y_2-y_1)V_0^2 , \tag{26}$$

$$\langle n_r\rangle=(y_2-y_1)\Gamma(0) , \tag{27}$$

where the iterative kernel of the integral equation, $\Gamma^{(k)}(y_1,y_2)$ satisfies

$$\Gamma^{(1)}(y_1,y_2)=\Gamma(y_1-y_2) , \tag{28}$$

$$\Gamma^{(k)}(y_1,y_2)=\int_{y_1}^{y_2}\Gamma(y_1,y)\Gamma^{(k-1)}(y,y_2)dy,\quad k\geq 2 , \tag{29}$$

We shall now take the correlation function as stationary with the $\Gamma(\tau)$ given by

$$\Gamma(y_1,y_2)=\Gamma_0 e^{-i\omega_r(y_1-y_2)}\Gamma(y_1-y_2) , \tag{30}$$

where $\Gamma(y)$ is a slowly varying function of y. ω_r, the mean frequency of the random component, is taken to coincide with the frequency ω_c of the coherent field. This assumption has been made quite often in many phenomenological analyses of Bose-Einstein correlation function[14] and is consistent with experimental data. As we shall demonstrate later, this assumption is also consistent with the multiplicity analysis presented in the later section. We do not have any strong theoretical justification for this choice except its simplicity. For the important special case of a Lorentzian autocorrelation function

$$\Gamma(y)=e^{-\tau|y|} , \tag{31}$$

the integration can be carried out. Explicit evaluation is given in the work of Jaiswal and Mehta.[26] For example, for the interval $\Delta_y=y_2-y_1$,

$$B_1=\bar{B}_1=1 , \tag{32}$$

$$B_2=(e^{-2\beta}+2\beta-1)/(2\beta^2) , \tag{33}$$

$$\bar{B}_2=2(e^{-\beta}+\beta-1)/(\beta^2) , \tag{34}$$

where

$$\beta=\tau\Delta_y .$$

Lower-order moments are relatively easy to calculate, and are available in the literature. Explicit expressions and properties of the higher orders are, however, rather involved. Our detailed evaluations and discussions up to the eighth μ_8 moments are reported elsewhere in a different article.[41]

C. Limiting cases

1. Chaotic limit

In the case of a totally chaotic source $[V_c(y)=0]$ and the Lorentzian correlation profile for $V_r(y)$, an analytic expression of the generating function $G(x)$ is given by[22]

$$G(x)=e^{\beta}\left[\cosh(z)+\frac{1}{2}\left[\frac{\beta}{z}+\frac{z}{\beta}\right]\sinh(z)\right]^{-1} , \tag{35}$$

where

$$z=(\beta\langle n_r\rangle x+\beta^2)^{1/2} .$$

A detailed derivation of this expression can be found in Ref. 42. It is worth mentioning that in the limit of vanishing Δ_y the above expression takes the form

$$G(x)=\frac{1}{1+\langle n_r\rangle x} . \tag{36}$$

Thus for a very small rapidity window, the limit of the P_n distribution is a negative binomial (NB) of $k=1$. This is to be compared with the limit of the classical processes, where the P_n is constructed from the Poisson distribution as the fundamental subprocess. P_n then tends to a Poisson distribution instead.

2. Total coherent limit

In the limit of vanishing chaotic component, $\langle n_r \rangle = 0$, each component of ϕ_j contributes as a Poisson distribution. Since the convolution of Poisson distributions is again a Poisson distribution, the overall distribution of P_n is Poissionian for any given $\langle n_c \rangle$.

3. Limit of vanishing rapidity window

With coherent component present, a closed expression for P_n is not known. We can, however, examine the limiting case of a very small β. To the first order of β, it is possible to show that, for $k > 1$,

$$B_k = 1 - \tfrac{1}{3}k\beta + A(\beta^2) ,$$
$$\bar{B}_k = 1 - \tfrac{1}{3}(k-1)\beta + A(\beta^2) . \tag{37}$$

Substituting the above expression into Eq. (23), we obtain

$$H(x) = -x\langle n_r \rangle - x\langle n_c \rangle + \sum_{k=2}^{\infty} (-x\langle n_r \rangle)^k \left[\frac{1}{k}(1 - \tfrac{1}{3}k\beta) + \frac{\langle n_c \rangle}{\langle n_r \rangle}[1 - \tfrac{1}{3}(k-1)\beta] \right] . \tag{38}$$

The summation can be easily performed; we then get

$$G(x) = \frac{1}{1+\langle n_r \rangle} \exp\left[-\frac{\langle n_c \rangle x}{1+\langle n_r \rangle} - \frac{\beta}{3} \frac{(\langle n_r \rangle + \langle n_c \rangle)x^2}{(1+\langle n_r \rangle)^2} \right] . \tag{39}$$

Thus the limit distribution for the situation of a vanishing rapidity window y is very similar to a PCLD distribution.

4. $\beta = \infty$ limit

In the limit of a finite correlation length but a very large rapidity window one obtains the limit $\beta = \infty$. In this situation the moment generating function $G(x)$ can be approximated by

$$G(x) = \exp\left[-\frac{1}{\beta}(\langle n_r \rangle + \langle n_C \rangle)x \right] + A(\beta^{-2}) . \tag{40}$$

The corresponding P_n distribution is also a Poisson distribution, and the KNO function $\psi(z) = \delta(z-1)$.[43] Since this behavior is opposite to what is observed empirically,[44,45] we may conclude that either the correlation length $1/\tau = \Delta_Y/\beta$ is increasing with Y so that β does not tend to infinity, or other fluctuation factors such as inelasticity or impact parameter may become the dominating factor of the overall P_n distribution.[34,3,46]

D. Joint multiplicity distributions in disjoint regions

In order to explore the inherent properties of correlation in P_n, we need to further divide the physical region of interest in different regions. This enables us to study the global correlations between these regions. The formal structure of the N-fold joint photon distribution with Gaussian light was first studied by Bedard.[22] Later on Mehta and Mista extended the formulation to partial coherent sources.[27] However, the resultant expressions for partial coherent sources are confined to a factorial cumulant. It is rather difficult to apply the formulation to the actual joint probability distributions or correlation parameters measured in hadronic physics. We shall therefore review some of the basic ingredients of the JM formulation to indicate how the formulation is applied directly to the joint probability distributions and various correlation measures. Let us first divide the region (y_1, y_2) into a forward region F $(0, y_2)$ and a backward region B $(y_1, 0)$. For N_F particles in the forward region, and N_B particles in the backward region, the joint distribution $P(N_F, N_B)$ is then given by

$$P(N_F, N_B) = \left\langle \frac{W_F^{N_F}}{N_F!} e^{-W_F} \frac{W_B^{N_B}}{N_B!} e^{-W_B} \right\rangle_{\text{ensemble}} , \tag{41}$$

where

$$W_F = \int_0^{y_2} I(y)dy, \quad W_B = \int_{y_1}^{0} I(y)dy . \tag{42}$$

The formulation in Sec. II A is a special case of the above equation. For example, convolution of the forward and backward regions leads to the overall distribution

$$\begin{aligned} P(N_S) &= \sum_{F,B} P(N_F, N_B)\delta(N_F + N_B - N_S) \\ &= \sum_{F,B} \left\langle \frac{W_F^{N_F}}{N_F!} e^{-W_F} \frac{W_B^{N_B}}{N_B!} e^{-W_B} \right\rangle_{\text{ensemble}} \\ &\quad \times \delta(N_F + N_B - N_S) \\ &= \left\langle \frac{(W_F + W_B)^{N_S}}{N_S!} e^{-W_F - W_B} \right\rangle_{\text{ensemble}} . \end{aligned} \tag{43}$$

Since

$$W_F + W_B = \int_{y_1}^{y_2} I(y)dy ,$$

$P(N_S)$ is the same as P_n given previously in Eq. (1). In quantum optics, there have been analogous formulations for photon counting by multiple detectors. These discussions were traditionally along the lines of the moment generating functions of P_n. From these complicated analyses relatively few insights can be obtained for the purpose of investigation of hadron multiplicity distributions. It is therefore necessary to consider an alternative approach of constructing the amplitudes and the probability directly. In order to do this, we need to construct the eigenfunctions $\phi_m(y)$ and the eigenvalues λ_m of Eq. (12).[18] They are states with definite parity,

$$\phi_m^{(\pm)}(y)=C[\exp(ik_m^{(\pm)}y)\pm\exp(-ik_m^{(\pm)}y)]/2 , \quad (44)$$

$$\lambda_m^{(\pm)}=\frac{2\beta\Delta_y}{\beta^2+(k_m^{(\pm)}\Delta_y)^2} , \quad (45)$$

where C is chosen for appropriate normalization. $k_m^{(\pm)}$ satisfies the self-consistency equation[18]

$$x^{(\pm)}=k_m^{(\pm)}\Delta_y/2 , \quad (46)$$

$$\frac{\beta}{x^{(\pm)}}=\pm[\tan(x^{(\pm)})]^{\pm 1} , \quad (47)$$

where the $\pm$ sign corresponds to eigenfunctions with the $\pm$ parity in Eq. (44). The above equations indicate that the higher-order terms of Eq. (15) contribute progressive less to the overall probability distributions and the associated cumulants. Their determination is limited by the statistics and uncertainties in the experimental data. Starting from the largest value of λ_k we have experimented with the convergence of the expansion in Eq. (15) to determine the minimum number of Gaussian terms that are needed to determine the probability P_n. This is done by comparing the resultant $\langle N_S \rangle$ and the cumulants μ_k up to the fourth order and requiring agreement with the theoretical prediction of Eq. (23) to 5%. (The value of the smallest eigenvalue λ_k reached about 0.0001.) We notice that the number of the eigenfunctions that significantly contribute to P_n is related to $\langle n \rangle$. With increasing $\langle n \rangle$, more and more eigenfunctions are needed. Typically the smallest eigenvalue we have used in this work is taken as 10^{-3}. Once an appropriate number of terms is determined, it is a straightforward matter to perform a Gaussian ensemble average over the functional space to build a sample of $P(N_F,N_B)$. Possible systematic and statistical errors are also estimated in sample Monte Carlo runs with increasing numbers of eigenvalues and sample size. A typical number of eigenfunctions up to 80 was used for the NA22 data with a Monte Carlo simulation with 50 000 trials. (Here a trial is identified by an individual set of random $\{C_m\}$.) In other words, the underlying hadronic field for NA22 is represented by a Gaussian ensemble of 80 eigenfunctions. With each Gaussian component of $\{C_m\}$ generated in a Monte Carlo program, the resultant stochastic field, and its integrated intensity W is a stochastic variable changing from trial to trial. Furthermore, the stochastic variables W_F and W_B are Poisson transformed according to Eq. (41) to give a complete table of the associated joint forward-backward multiplicity distributions. The accumulated ensemble of all the tables is the final joint probability distribution $P(N_F,N_B)$. Its properties are compared with experimental data in Sec. III. At higher collider (UA5) energies, a typical number of eigenfunctions used for 546 GeV increases to more than 100.

Two quantities are commonly used to characterize the nature of the correlation within the joint distribution function $P(N_F,N_B)$. The first is the forward-backward correlation for a fixed N_F. Let us introduce the conditional probability distribution $P_F(N_B|N_F)$:

$$P_F(N_B|N_F)=P(N_F,N_B)\Big/\sum_B P(N_F,N_B) . \quad (48)$$

Various moments of $P_F(N_B|N_F)$ can then be evaluated. For example,

$$\langle N_B \rangle_F=\sum_B N_B P_F(N_B|N_F) . \quad (49)$$

Empirically it is found that for a substantial region of N_F, the above equation is approximately a linear function of N_F.[36,37,45] Thus we may write

$$\langle N_B \rangle_F=a+bN_F . \quad (50)$$

The slope parameter b is often given empirically in the literature.

Another interesting subject is the properties of the conditional probability distribution of N_F with a fixed $N_S=N_F+N_B$. The purpose of such consideration is to compare a quantum statistical model having inherent correlations with classical models without correlations (leading to random partitions and binomial distributions of a single particle). We start with the conditional distribution with a fixed N_S,

$$P_S(N_F|N_S)=\frac{P(N_F,N_B=N_S-N_F)}{\sum_{F,B} P(N_F,N_B)\delta(N_F+N_B-N_S)} . \quad (51)$$

For a classical random partition of individual particles, the corresponding distribution is a binomial (BN) distribution

$$B_S(N_F|N_S)=P_S^{(1)}(N_F|N_S)$$
$$=\frac{N_S!}{N_B!N_F!}f^{N_F}(1-f)^{N_B}\delta(N_F+N_B-N_S) , \quad (52)$$

where f is the probability that an individual hadron fall into the forward region ($f=\frac{1}{2}$ for symmetrical regions.) This BN distribution can be characterized by

$$\langle N_F \rangle_S=\sum_F N_F P_S(N_F|N_S)$$
$$=fN_S , \quad (53)$$

and a reduced second moment C_{eff} (which characterizes the effective size of clustering[45,47]),

$$C_{\text{eff}}=\frac{4D_S^2}{N_S} \quad (54)$$

with D_S^2 being the dispersion of N_F with fixed N_S:

$$D_S^2=\langle N_F^2 \rangle_S-\langle N_F \rangle_S^2$$

For the case of the production of single particle with random partition between a symmetrical forward and backward region $f=\frac{1}{2}$. We get $\langle N_F \rangle = N_S/2$, and naturally, the size of the cluster [Eq. (53)],

$$C_{\text{eff}}=1 \ .$$

Similarly, for particles being created in clusters of size 2, the forward-backward distribution is

$$P_S^{(2)}(N_F|N_S)=\frac{N_S/2!}{(N_B/2)!(N_F/2)!}f^{N_F/2}(1-f)^{N_B/2} \times \delta(N_F+N_B-N_S) \ , \tag{55}$$

$$C_{\text{eff}}=2 \ .$$

The above situation can be refined to include a finite correlation length of clustering in the probability P_n along the rapidity axis. A center cluster may then be partially in the forward and partially in the backward region. C_{eff} then need not be an integer.

In the quantum statistical formulation of Eqs. (4) and (43), not only is the effective cluster size greater than 1, C_{eff} is also a function of N_S. In a previous analysis of the UA5 data, the values of C_{eff} indicated the need of using clusters of size between 2 and 3. Thus the quantum statistical approach with a finite correlation length suggests an effective cluster size somewhat different from the classical approach where the correlation length of the field was ignored.[45,48]

As we shall discuss in the following section, the unique description of the $P(N_F,N_B)$ distribution for the entire region, as well as for the correlations between different regions provides much better determination of the parameters needed in our formulation.

III. PHENOMENOLOGICAL ANALYSIS

In this section we shall explore the nature of the multiplicity distribution within the freedom of the three parameters mentioned earlier. We shall restrict ourselves to the non-single-diffractive (NSD) multiplicity distributions of the NA22 and the ISR data, in order to explore the nature of the multiplicity distributions implicitly constructed through quantum statistical correlation. Many potentially important considerations such as the conservation of charge and the inelasticity fluctuations are ignored in the present formulation. Throughout this section, we shall abbreviate N_S by n, whenever there is no ambiguity. We start by adopting a procedure similar to the recent work of Fowler *et al.*[34] In this procedure, the first parameter $\langle n \rangle$ is fixed easily by the experimental value. We then require that μ_2 calculated through Eq. (23) also agree with the experimental values. Since there are altogether three free parameters, one more condition is needed. For a given correlation parameter β, we shall then calculate the forward-backward slope b. Since the b is rather sensitive to β, all the parameters are uniquely determined. This in turn determines the entire joint distribution $P(N_F,N_B)$.

Notice that we have not compared higher moments μ_k of the multiplicity distribution $P(n)$. Unless the JM representation in general has the correct form, the requirement that $\langle n \rangle$ and μ_2 taking the experimental value would not guarantee a correct overall distribution in $P(n)$.

A. $P(N_S)$ distribution

The phenomenological representation used here contains three parameters: the strength of a coherent component $\langle N_c \rangle$, the strength of a chaotic component $\langle N_r \rangle$, and a reduced correlation length β of the chaotic component. In other words, the probability distributions are characterized by three parameters: the overall average multiplicity

$$\langle n_S \rangle = \langle n_c \rangle + \langle n_r \rangle \ ,$$

chaoticity

$$p=\frac{\langle n_r \rangle}{\langle n_S \rangle}$$

characterizing the noise content, and the relative correlation length

$$\beta=\tau\Delta_y$$

of the chaotic component. Once these three parameters are determined, we have a unique description of the $P(N_F,N_B)$ distribution for the entire region, as well as for the correlations between different regions. Thus the total multiplicity distributions for a fixed rapidity window, and the joint multiplicity distributions between different windows are completely specified. We are now in a position to determine these parameters from the experimental data. Given a set of experimental values of $P(n)$, from NA22 or ISR pp data,[35,36] the values of $\langle n \rangle^{\text{expt}}$ and μ_2^{expt} lead to a constraint between the chaoticity parameter p and the correlation parameter β. Figure 1 shows these

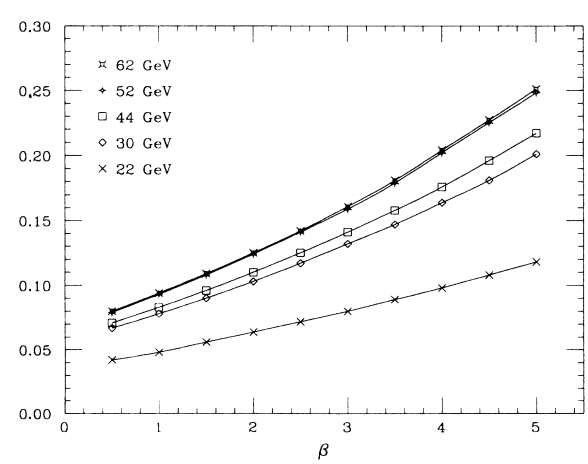

FIG. 1. Relationships between chaoticity p and β that lead to the correct values of $\langle n_S \rangle_{\text{expt}}$ and $\mu_{2,\text{expt}}$. Curves from top to bottom correspond to the ISR energies of 62, 52, 44, and 30 GeV (Refs. 36 and 37) and the NA22 energy of 22 GeV (Ref. 35).

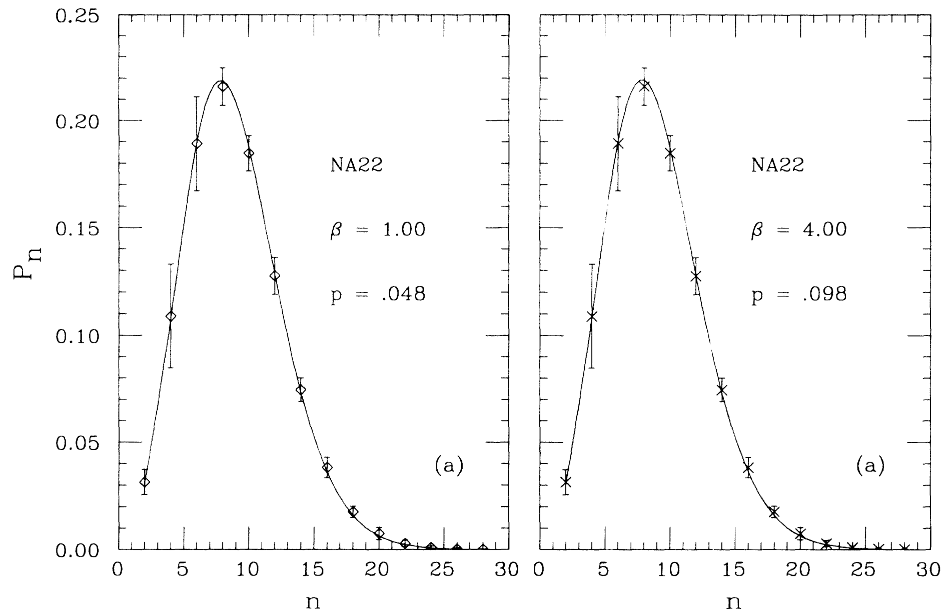

FIG. 2. Explicit values of P_n as a function of n at the NA22 energy, (Ref. 35), with the correlation parameter β arbitrary taken: (a) $\beta=1$, $p=0.048$ and (b) $\beta=4$, $p=0.078$.

relationships at the NA22 and ISR energies. Let us first examine the sensitivity of the total distribution, $P(n)$, to the various values of p and β along the curve of constraint. In principle, the overall shape of the $P(n)$ distribution alone may be sufficient to determine both values of β and p, since information beyond the values of $\langle n \rangle^{\text{expt}}$ and μ_2^{expt} are included.

To examine this possibility, we have plotted in Fig. 2(a) the explicit values of the $P(n)$ at the NA22 energy with the correlation parameter β arbitrarily taken to be $\beta=1$. Here the overall normalization is chosen so that the sum over all even prong events is 1. When this phenomenological representation is compared with the experimental data, the agreement is surprisingly good. We obtain a total chi-square $\chi_r^2=2.41$ for 11 degrees of freedom. We would like to emphasize that the χ^2 indicated here include all the available P_n. Thus our fit is very satisfactory even for the extreme tails of the P_n distribution. To dramatize the lack of uniqueness in determining the parameter β, we also present in Fig. 2(b) the same plot with a rather large correlation length $\beta=4$, and still obtain a value of total $\chi_r^2=2.42$. The difference between Figs. 2(a) and 2(b) is nearly indistinguishable (as reflected by the total χ_r^2). We may therefore conclude that as long as p and β together give the proper values of the second moment μ_2, the total multiplicity distribution $P(n)$ is very insensitive to the individual values of p and β.

The very small value of the total χ_r^2 and the very large uncertainty in the determination of β and p separately, implies that we need not be overly concerned about the consequences of the experimental uncertainties in $\langle n \rangle^{\text{expt}}$ and μ_2^{expt} (the quantities are typically known to 10% or better and can be used to determine a narrow corridor along each curve of Fig. 1). Such considerations modify the constraints between the control parameter β and p slightly, and do not change the main conclusions of this paper.

The situation of the ISR data is rather comparable with what is observed at NA22 energy. On each of the curves of constraint (where the values of p and β reproduce $\langle n \rangle$ and μ_2,) reasonable phenomenological fits of P_n can be obtained at each ISR energy. Table I summa-

TABLE I. Typical phenominological fits to the multiplicity distribution P_n at NA22 and ISR energies.

Energy (GeV)	$\langle n \rangle$	$\mu_2/\langle n \rangle^2$	β	p	χ^2/N_{DF}
22	8.93	0.07	1.0	0.048	2.4/10
			4.0	0.064	2.4/10
30	10.7	0.11	1.0	0.078	8/11[a]
44	12.2	0.17	1.0	0.083	9/15
52	12.8	0.13	1.0	0.093	8/16
62	13.6	0.13	1.0	0.094	17/16

[a] $n=2$ data point not included.

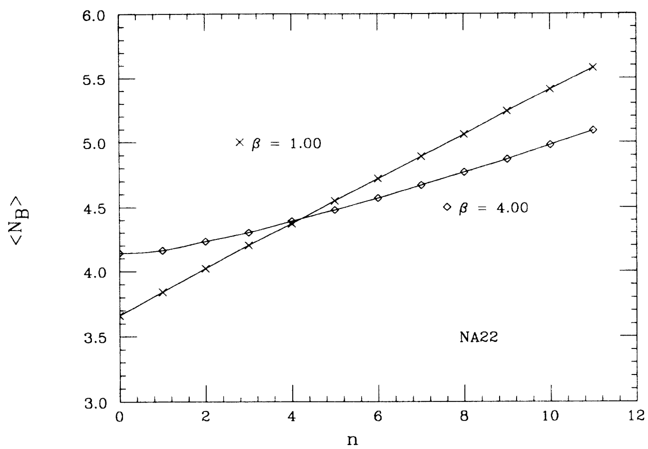

FIG. 3. Using the same parametrization as given in Fig. 2 for the joint forward-backward probability distribution $P(N_F,N_B)$, $\langle N_B \rangle$ is shown as a function of N_F at the NA22 energy for (a) $\beta=1$ and for (b) $\beta=4$.

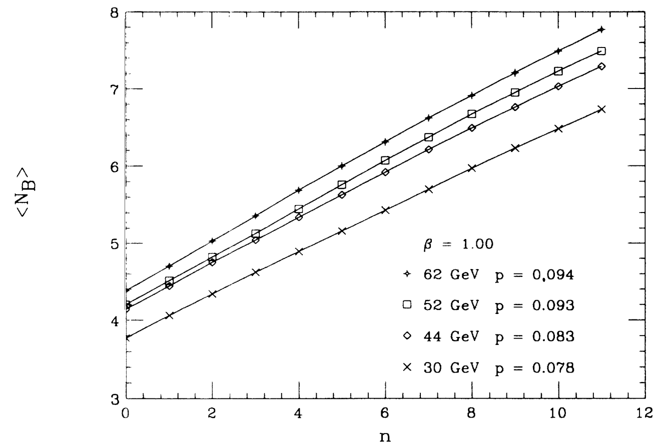

FIG. 5. Given the same parameters as in Fig. 4, the corresponding $\langle N_B \rangle$ is shown as a function of N_F at the ISR energies: (a) 30 GeV, (b) 44 GeV, (c) 52 GeV, and (d) 62 GeV.

rizes the values of $\chi^2/N_{\rm DF}$ for some of the typical values of β. More detailed comparison with the experimental $P(n)$ shall be presented later for specific values of β determined through the forward-backward correlation slope parameter b.

B. Forward-backward correlation

As we mentioned earlier, to determine more specifically the parameters, it is necessary to use correlation properties between the forward and backward regions. Figure 3 plots the $\langle N_B \rangle$ as a function of N_F at NA22 energy, for the same parametrization as given in Fig. 2 [$\beta=1$, $p=0.048$ in (a), and $\beta=4$, $p=0.078$ in (b)]. Notice that for the whole region of N_F the $\langle N_B \rangle_F$ dependence is almost a straight line. Thus the value of b allows us to select a correlation parameter β and a chaoticity parameter p. The forward-backward slope can therefore be used as a possible tool to discriminate solutions that cannot be obtained by examining the overall KNO plots alone. Similar analysis can also be applied to the ISR data. Figures 4(a)–4(d) present the comparisons between $P(n)$ and experimental data. We notice that for all the energies, the $\chi^2/N_{\rm DF}$ are acceptable (except possibly the $n=2$ components, P_2 has therefore been excluded). Similarly, Figs. 5(a)–5(d) present the $\langle N_B \rangle_F$ dependence on N_F. The role of the forward-backward correlation can be clearly seen. Figures 6 summarize the dependence of the

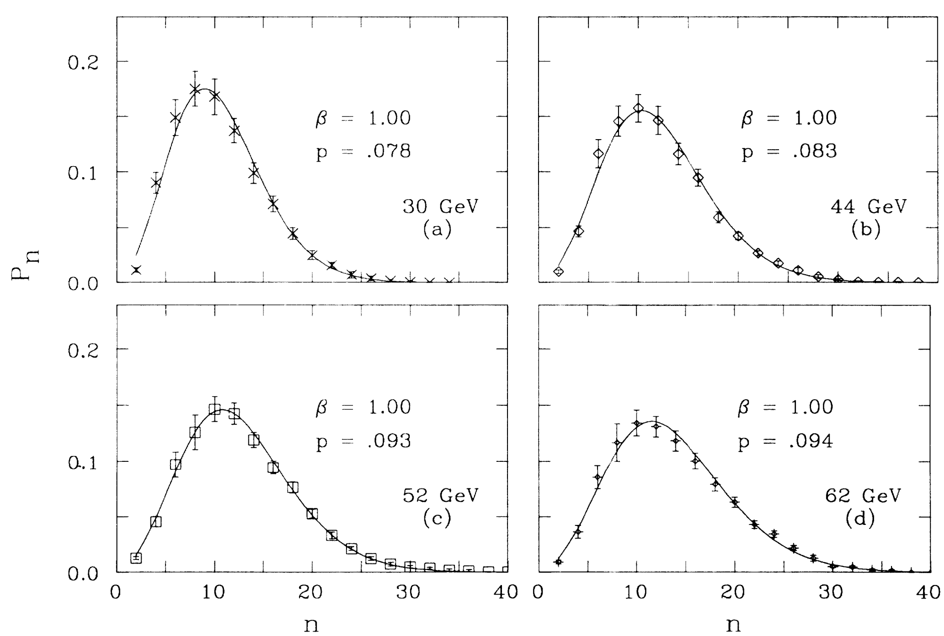

FIG. 4. Explicit values of the P_n as a function of n at the ISR energies: (a) 30 GeV, (b) 44 GeV, (c) 52 GeV, and (d) 62 GeV with the correlation parameter β arbitrary taken to be $\beta=1$, and the associated values of the chaoticity parameter p as labeled.

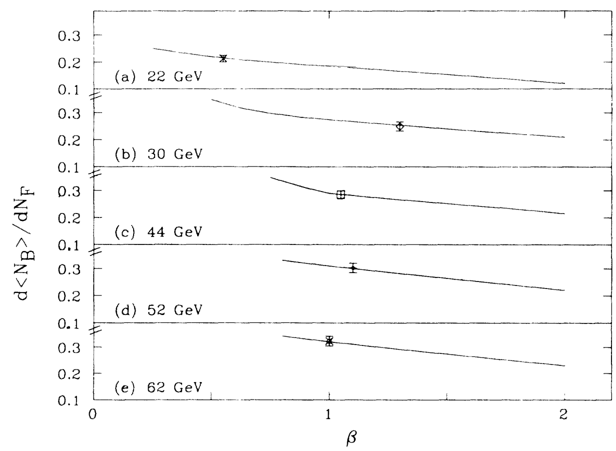

FIG. 6. Forward-backward slope $d\langle N_B\rangle/dN_F$ is shown as a function of the correlation parameter β at different energies as labeled: (a) 22 GeV, (b) 30 GeV, (c) 44 GeV, (d) 52 GeV, and (e) 62 GeV. The estimated experimental data point (with error bar) on each curve can be used to determine the corresponding value of the corresponding correlation length β.

forward-backward slope as a function of the correlation parameter β. In this figure, we also indicated how the experimental values of the forward-backward slopes can be used to determine the values of β for the NA22 and ISR data. Notice that the values of β is close to 1 for all the energies.

Even though precise values for the forward-backward parameters are not available for NSD data, the value of the slope parameters presented here are quite consistent to typical values obtained in the NA22 and ISR region. We also notice that in the recent NA22 analysis, the slope parameter is a sensitive function of the selection of charge of the final state. This indicates that charge consideration plays an important role in correlation. Further extension of our present analysis to the charge space is needed.

C. Effective clustering and binomial distribution

In order to demonstrate the forward-backward correlation, we have also evaluated a quantity

$$P_S'(x_F|N_S)=cP_S(N_F|N_S)/B_N(N_F|N_S) \tag{56}$$

with

$$x_F=\frac{N_F}{N_S} \tag{57}$$

where c is the normalization constant so that $P_S'(\frac{1}{2}|N_S)=1$. Figure 7 plots $P_S'(x_F|N_S)$ at NA22 energy with $\beta=1$ and fixed $N_S=5$. Since $P_S'(x_F|N_S)\neq 1$, the corresponding $P_S(N_F|N_S)$ is not a binomial distribution. The deviation of $P_S'(x_F|N_S)$ from 1 also varies as a function of N_S. This dependence is summarized in Fig. 8, where we have plotted $C_{\rm eff}$ (defined by $4D_S^2/N_S$) as a function N_S. Figure 8 also presents similar dependence at the ISR energies for the same parametrization ($\beta=1$ used in Fig. 4.)

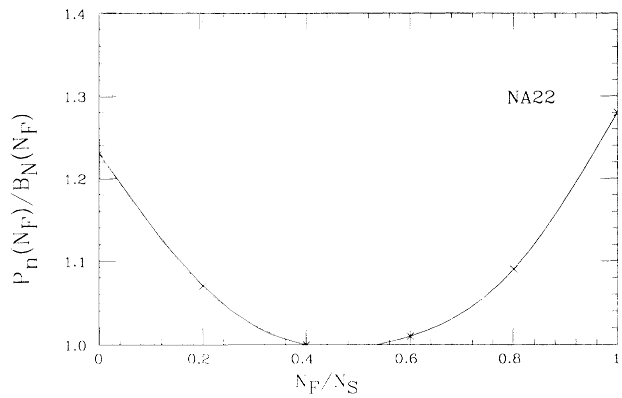

FIG. 7. $P_S'(x_F|N_S)=P_S(N_F|N_S)/B_N(N_F|N_S)$ as a function of $x_F=N_F/N_S$ with fixed $N_S=5$ for $\beta=1$ at NA22 Energy.

D. Correlation and energy dependence

The energy dependence in the KNO distribution $\psi(z)=\langle n\rangle P_n$, $z=n/\langle n\rangle$, is traditionally of interest. Empirically, the KNO function is a slowly widening function of W. Notice that the reduced factorial cumulants

$$\mu_k'=\mu_k/\langle N_S\rangle^k$$

are functions of p and β, and are independent of $\langle N_S\rangle$. The widening of the KNO function should therefore be reflected either through an increase in p or an increase in β. Figure 9 plots the value of p determined earlier as a function of W. It indicates that not only are the absolute values of the $\langle n_r\rangle$ of the chaotic components and the $\langle n_c\rangle$ of the coherent components increasing, the relative amount of the chaotic component p is also slowly increas-

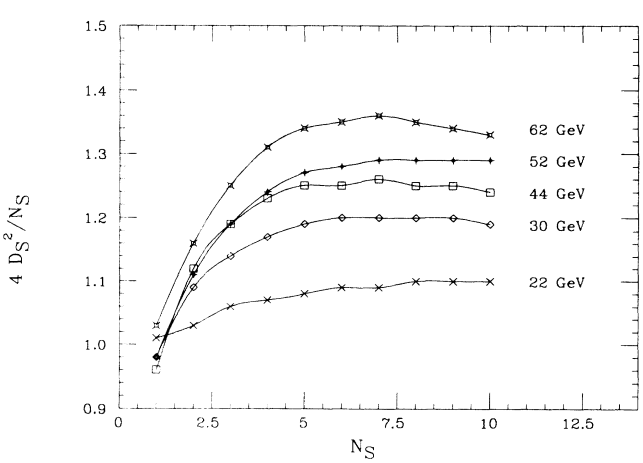

FIG. 8. The effective cluster size, $C_{\rm eff}=4D_s^2/N_s$, as a function of N_S for $\beta=1$ at different energies as labeled: (a) 22 GeV, (b) 30 GeV, (c) 44 GeV, (d) 52 GeV, and (e) 62 GeV. The parameters are as indicated in Figs. 3 and 4.

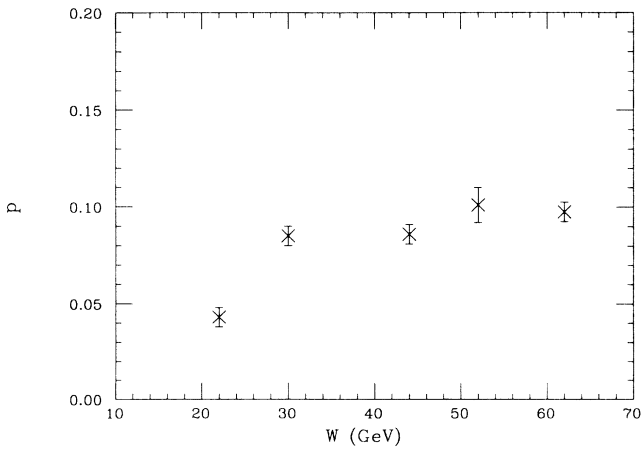

FIG. 9. Value of chaoticity parameter p as a function of center-of-mass energy W.

ing as a function of the total energy W. On the other hand, the relative correlation parameter β remains more or less a constant. Since the total width of the rapidity plateau Δ_y is increasing as a function of W, the absolute correlation length $1/\tau=\Delta_y/\beta$ is also increasing as a function of Δ_y.

IV. CONCLUSION

In this paper we have presented a phenomenological representation of the hadronic multiplicity data in the framework of a quantum statistical system with correlation. Our basic formulation is essentially the same as the Jaiswal-Mehta formulation developed earlier in quantum optics. However, the explicit evaluation of the multiplicity distribution for a single window and the joint multiplicity distributions for two regions are new. In fact, this is one of a very few quantum statistical models where the global joint multiplicity distributions are calculated explicitly. These global probability distributions have also been compared directly with the experimental data in a detailed phenomenological analysis (instead of an indirect comparison through the factorial cumulants[49]).

The phenomenological representation used here contains three parameters: the strength of a coherent component $\langle N_c \rangle$, the strength of a chaotic component $\langle N_r \rangle$, and a reduced correlation length β. Both the total multiplicity distributions for a fixed rapidity window and the joint multiplicity distributions between different windows are completely specified. Since joint multiplicity distributions are in general not available from experiment, we have calculated only the total multiplicity distribution (nonsingle diffractive) for the whole rapidity window, the forward-backward correlation slope parameter, and the effective size of the cluster (of random partition between the forward and backward region).

Within the Jaiswal-Mehta framework of quantum statistical formulation for a Lorentzian correlation spectrum, the overall distribution P_n appears to be quite consistent with experimental data. However, this comparison of P_n does not determine uniquely the three parameters that are needed to specify a phenomenological representation. We noticed that, as long as a combination of $\langle n_c \rangle$, $\langle n_r \rangle$, and β lead to the experimental values of $\langle n \rangle$ and μ_2, it is possible to obtain without difficulties the experimental P_n with a reasonable χ^2/N_{DF}. This suggests that the Jaiswal-Mehta formulation provides a good starting point as a quantum statistical description of the hadronic production processes.

In general, the forward-backward slope parameter b is sensitive to the nature of correlation. The same is true in the Jaiswal-Mehta formulation. By requiring a phenomenological JM representation to possess a reasonable forward-backward slope, β can be determined to be close to 1 throughout the region of NA22 to ISR energies. The corresponding values of p on the other hand is slowly increasing with $\langle n \rangle$. Preliminary studies at the collider energy indicate that this feature continues. At Collider energies, the values of $\langle n \rangle$ are much larger than at the ISR energies. This makes the convergence of the eigenfunctions expansion of Eq. (1) very slow, and the numerical evaluations of the high-P_n region much more difficult. Detailed analysis will be reported later.

A comprehensive analysis is under way to evaluate the present formulation of the multiplicity distribution as a function of the rapidity window. Notice that for the JM formulation to be attractive and economical, one should be able to use a single correlation length to describe $P(N_F,N_B)$ for a large width of the window. It should then replace the use of k of the empirical NB distribution as a function of the rapidity window. For example, the widening of the KNO plot for decreasing rapidity window width should be a reflection of the decrease in β. Indeed, for $\beta=\infty$, the present formulation predicts a limiting KNO distribution of a NB with $k=1$. Our preliminary analysis of the NA22 data at $Y\leq 1$ and UA5 data at $\eta \leq 1.0$ indicates that the multiplicity distribution can be adequately described prior to the introduction of the fluctuation due to inelasticity. Since these analyses are more interesting but complicated, we shall refer the discussion to the recent work of Fowler *et al.*,[49] where the factorial cumulants are used as the primary tool of analysis.

Even though the formulation reported in this paper has no difficulty reproducing the NSD multiplicity distribution for a wide range of energies, various considerations that we have ignored may eventually change the values of the final parametrization. This includes, for example, the inelasticity and leading particle effects, nonstationary effects, and the consideration of charge and energy.

Throughout this paper we have used amplitude correlations of an effective charged field π_{ch}. In a more comprehensive formulation, one needs to introduce at least two fields, π_+ and π_-. Charge conservation should also be properly incorporated. It would be easier to consider only one type of charge, say the π_- sector. There are, however, relatively little data available for a comprehensive analysis. Data on P_n at NA22 and UA1 in the near future will be very helpful for further evaluation of the merit of the quantum statistical approach reported here.

Recently we have generalized the current quantum statistical formulation for factorial cumulants to include a

p_T spectrum, and a nonstationary rapidity distribution, as well as charge correlations. It is, however, still difficult to construct the probability distribution explicitly in these generalizations. Work along this line is in progress.

ACKNOWLEDGMENTS

This research was supported in part by National Science Foundation Grant No. NSF PHY-8703726, a supplementary NSF Grant for the Supercomputer usage at the Cornell Supercomputing facility, as well as by The Science Alliance, a State of The Tennessee Center of Excellence at the University of Tennessee, Knoxville. The author wishes to thank Dr. P. Carruthers, Dr. R. M. Weiner, Dr. E. M. Friedlander, Dr. L. Van Hove, Dr. R. C. Hwa, Dr. C. S. Lam, Dr. T. Meng, Dr. G. Wilk, and Dr. M. Biyajima for useful discussions. He wishes to thank the Department of Physics, University of Arizona and the Department of Physics, University of Marburg, for their hospitality during a sabbatical leave, where the final version of this paper was prepared. He also wishes to thank the Deutsche Forschungsgemeinschaft for their support at the University of Marburg.

---

[1]P. Carruthers and C. C. Shih, Mod. Phys. A **2**, 1544 (1987).
[2]R. M. Weiner, Z. Phys. C **38**, 199 (1988).
[3]R. C. Hwa, in *Multiparticle Production*, proceedings of the Shandong Workshop, Jinan, Shandong, China, 1987, edited by R. C. Hwa and Qu-bing Xie (World Scientific, Singapore, 1988).
[4]A. Bialas and R. Peschanski, Phys. Lett. B **207**, 59 (1988).
[5]P. Dahlqvist, B. Andersson, and G. Gustafson, Phys. Lett. B **202**, 365 (1988).
[6]P. Carruthers, E. M. Friedlander, C. C. Shih, and R. M. Weiner, Phys. Lett. B **222**, 487, (1989).
[7]A. Capella, K. Fialowski, and A. Krzywicki, Phys. Lett. B **230**, 149 (1989).
[8]P. Carruthers and I. Sarcevic, Phys. Rev. Lett. **63**, 1562 (1989).
[9]E. A. De Wolf, Acta Phys. Pol. (to be published).
[10]B. Andersson *et al.*, Phys. Rep. **97**, 31 (1983); B. Andersson and W. Hoffmann Phys. Lett. **169B**, 364 (1986).
[11]A. Capella, J. Kwiecinski, and J. Tran Than Van, Phys. Rev. Lett. **58**, 2015 (1987).
[12]P. Aurenche and F. W. Bopp, Z. Phys. C **13**, 459 (1982).
[13]W. R. Chen and R. C. Hwa, Phys. Rev. D **36**, 760 (1987).
[14]G. N. Fowler *et al.*, Phys. Rev. D **37**, 3127 (1988).
[15]L. Mandel, Proc. Phys. Soc. London **74**, 233 (1959).
[16]R. J. Glauber, in *Physics of Quantum Electronics*, edited by P. L. Kelly, B. Lax, and P. E. Tamnwald (McGraw-Hill, New York, 1966), p. 788; R. J. Glauber, in *Quantum Optics*, edited by R. J. Glauber (Academic, New York, 1969), p. 15.
[17]G. Lachs, Phys. Rev. **138**, 1012 (1965).
[18]B. Saleh, *Photoelectron Statistics* (Springer, Berlin, 1978).
[19]J. Perina, *Coherence of Light* (Reidel, Dordrecht, 1985).
[20]C. D. Cantrell, Phys. Rev. A **3**, 728 (1971).
[21]T. Aoki, Phys. Rev. A **16**, 2432 (1977).
[22]G. Bedard, Phys. Rev. **161**, 1304 (1967).
[23]G. Lachs, J. Appl. Phys. **42**, 602 (1971).
[24]L. Mista, J. Perina, and V. Perinova, Phys. Lett. **35A**, 197 (1971).
[25]R. Horak, L. Mista, and J. Perina, Phys. Lett. **35A**, 400 (1971).
[26]C. L. Mehta and A. K. Jaiswal, Phys. Rev. A **2**, 2570 (1971).
[27]A. K. Jaiswal and C. L. Mehta, Phys. Rev. A **2**, 168 (1970).
[28]G. N. Fowler and R. M. Weiner, Phys. Lett. **70B**, 201 (1977); Phys. Rev. D **17**, 3118 (1978).
[29]B. Durand and L. O'Raifeartaigh, Phys. Rev. D **13**, 99 (1976).
[30]M. Gyulassy, S. K. Kauffmann, and L. W. Wilson, Phys. Rev. C **20**, 2267 (1979).
[31]C. C. Shih and P. Carruthers, Phys. Rev. D **38**, 56 (1988).
[32]C. C. Shih, Phys. Rev. D **37**, 3118 (1988).
[33]R. Szwed and G. Wrochna, Z. Phys. C **29**, 255 (1985), R. Szwed, G. Wrochna, and A. K. Wroblewski, Warsaw University IFD report, 1987 (unpublished).
[34]G. N. Fowler, E. M. Friedlander, R. M. Weiner, J. Wheeler, and G. Wilk, Phys. Rev. D **37**, 3127 (1988); University of Marburg report, 1966 (unpublished).
[35]NA22 Collaboration, M. Adamus *et al.*, Phys. Lett. B **177**, 239 (1986); W. Kittel (private communication) for the P_n data.
[36]K. Alpgard, Phys. Lett. **123B**, 361 (1983).
[37]S. Uslig *et al.*, Nucl. Phys. **B132**, 132 (1978).
[38]E. M. Friedlander, X. C. He, C. C. Shih, and R. M. Weiner (unpublished).
[39]G. N. Fowler *et al.*, Phys. Rev. Lett. **56**, 2119 (1986).
[40]T. Sjostrand, Comput. Phys. Commun. **39**, 347 (1986); T. Sjostrand and M. Bengtsson, *ibid.* **43**, 367 (1987).
[41]C. C. Shih, University of Tennessee report, 1988 (unpublished).
[42]B. Saleh, *Photoelectron Statistics* (Springer, Berlin, 1978), p. 182.
[43]Z. Koba, H. B. Nielsen, and P. Olesen, Nucl. Phys. **B40**, 317 (1972).
[44]UA5 Collaboration, J. Alner *et al.*, Phys. Lett. **151B**, 309 (1985).
[45]UA5 Collaboration, J. Alner *et al.*, Phys. Lett. **167B**, 476 (1986).
[46]A. Giovannini and L. Van Hove, Z. Phys. C **30**, 391 (1986); L. Van Hove, in *Multiparticle Production* (Ref. 3).
[47]T. T. Chou and C. N. Yang, Phys. Lett. **135B**, 175 (1981).
[48]P. Carruthers and C. C. Shih, Phys. Lett. **165B**, 209 (1984).
[49]R. M. Weiner (private communication).